2018-10

Environmental Factors and Internal Processes Contributing to the Interrupted Rapid Decay of Hurricane Joaquin (2015)

Hendricks, Eric A.; Elsberry, Russell L.; Velden, Christopher S.; Jorgensen, Adam C.; Jordan, Mary S.; Creasey, Robert L.

American Meteorological Society

Hendricks, Eric A., et al. "Environmental Factors and Internal Processes Contributing to the Interrupted Rapid Decay of Hurricane Joaquin (2015)." Weather and Forecasting 2018 (2018).
https://hdl.handle.net/10945/60234

Environmental Factors and Internal Processes Contributing to the Interrupted Rapid Decay of Hurricane Joaquin (2015)

ERIC A. HENDRICKS

Department of Meteorology, Naval Postgraduate School, Monterey, California

RUSSELL L. ELSBERRY

Department of Meteorology, Naval Postgraduate School, Monterey, California, and Trauma, Health, and Hazards Center, University of Colorado Colorado Springs, Colorado Springs, Colorado

CHRISTOPHER S. VELDEN

Cooperative Institute for Meteorological Satellite Studies, Madison, Wisconsin

ADAM C. JORGENSEN, MARY S. JORDAN, AND ROBERT L. CREASEY

Department of Meteorology, Naval Postgraduate School, Monterey, California

(Manuscript received 31 December 2017, in final form 31 May 2018)

ABSTRACT

The objective in this study is to demonstrate how two unique datasets from the Tropical Cyclone Intensity (TCI-15) field experiment can be used to diagnose the environmental and internal factors contributing to the interruption of the rapid decay of Hurricane Joaquin (2015) and then a subsequent 30-h period of constant intensity. A special CIMSS vertical wind shear (VWS) dataset reprocessed at 15-min intervals provides a more precise documentation of the large ($\sim$15 m s^{-1}) VWS throughout most of the rapid decay period, and then the timing of a rapid decrease in VWS to moderate ($\sim$8 m s^{-1}) values prior to, and following, the rapid decay period. During this period, the VWS was moderate because Joaquin was between large VWSs to the north and near-zero VWSs to the south, which is considered to be a key factor in how Joaquin was able to be sustained at hurricane intensity even though it was moving poleward over colder water. A unique dataset of High Definition Sounding System (HDSS) dropwindsondes deployed from the NASA WB-57 during the TCI-15 field experiment is utilized to calculate zero-wind centers during Joaquin center overpasses that reveal for the first time the vortex tilt structure through the entire troposphere. The HDSS datasets are also utilized to calculate the inertial stability profiles and the inner-core potential temperature anomalies in the vertical. Deeper lower-tropospheric layers of near-zero vortex tilt are correlated with stronger storm intensities, and upper-tropospheric layers with large vortex tilts due to large VWSs are correlated with weaker storm intensities.

1. Introduction

Hurricane Joaquin (2015) was the strongest Atlantic hurricane with a nontropical origin in the satellite era (Berg 2016). Joaquin intensified rapidly while slowly moving southwestward toward the Bahamas over sea surface temperatures (SSTs) that were approximately 1.1°C higher than normal and became a major hurricane (category 3) at 0000 UTC 1 October 2015. Joaquin then reversed course on 2 October and moved to the north-northeast under the influence of a deep midlatitude trough over the southeastern United States (Berg 2016). While moving to the north-northeast, Joaquin intensified to 135 kt (1 kt $\approx$ 0.51 m s^{-1}) at 1200 UTC 3 October, but after 1800 UTC 3 October began to rapidly decrease in intensity (Table 1).

The focus of this study is the interruption of the extremely rapid decay of Hurricane Joaquin around 0000 UTC 5 October, and the subsequent constant intensity of 75 kt from 0000 UTC 5 October through 0600 UTC 6 October (Table 1). Whereas postrecurvature hurricanes typically decay as they move poleward over colder water,

Corresponding author: R. L. Elsberry, elsberrylr@comcast.net

DOI: 10.1175/WAF-D-17-0190.1

TABLE 1. Final best-track analysis of Hurricane Joaquin (2015) from Berg (2016) with Date Time Group (DTG), latitude, longitude, central pressure, and maximum sustained winds before, during, and after the interrupted decay at 0000 UTC 5 Oct with a period of constant maximum wind speed from 0000 UTC 5 Oct to 0600 UTC 6 Oct.

DTG	Lat (°N)	Lon (°W)	Pressure (mb)	Wind speed (kt)
0000 UTC 2 Oct	22.9	74.4	931	120
0600 UTC 2 Oct	23	74.7	935	120
1200 UTC 2 Oct	23.4	74.8	937	115
1600 UTC 2 Oct	23.6	74.8	940	110
1800 UTC 2 Oct	23.8	74.7	941	110
2100 UTC 2 Oct	24.1	74.5	942	110
0000 UTC 3 Oct	24.3	74.3	943	115
0600 UTC 3 Oct	24.8	73.6	945	120
1200 UTC 3 Oct	25.4	72.6	934	135
1800 UTC 3 Oct	26.3	71	934	130
0000 UTC 4 Oct	27.4	69.5	941	115
0600 UTC 4 Oct	28.9	68.3	949	105
1200 UTC 4 Oct	30.4	67.2	956	95
1800 UTC 4 Oct	31.6	66.5	958	85
0000 UTC 5 Oct	32.6	66	961	75
0600 UTC 5 Oct	33.6	65.6	964	75
1200 UTC 5 Oct	34.4	65.2	964	75
1800 UTC 5 Oct	35.3	64.5	964	75
0000 UTC 6 Oct	36.2	63.6	967	75
0600 UTC 6 Oct	37	62.3	970	75
1200 UTC 6 Oct	37.9	60.4	974	70

the 60-kt decay from a maximum intensity of 135 to 75 kt just 36 h later is an extreme decay rate according to Wood and Ritchie (2015). Then for that decay to be suddenly interrupted, and for Joaquin to maintain an intensity of 75 kt for 30 h while accelerating poleward, is unusual as continued decay is normally expected over colder water in the absence of baroclinic effects that might have maintained the intensity.

Berg (2016) indicated that increasing northwesterly vertical wind shear (VWS) resulted in the onset of rapid weakening of Joaquin. The Statistical Hurricane Intensity Prediction Scheme (SHIPS; DeMaria et al. 2005) intensity forecasts from 0000 UTC 4 October to 0000 UTC 5 October (Fig. 1) underestimate the rapid weakening during the early forecast intervals. While these SHIPS intensity forecasts then somewhat coincidently had smaller errors during the subsequent constant intensity period, these SHIPS forecasts then indicate rapid weakening to 20 kt when the verifying intensities continued to be greater than 60 kt due to the 30-h period of constant intensity of Joaquin following the interrupted rapid decay.

The objective of this study is then to diagnose the environmental factors and internal processes that contributed to the interrupted rapid decay and the period of constant intensity. Jorgensen (2017) had demonstrated that among the Hendricks et al. (2010) environmental factors that best compared with the Joaquin intensity changes was the VWS from both the SHIPS and the CIMSS technique (Gallina and Velden 2002; Velden and Sears 2014). Whereas the SHIPS simply takes the difference between the Global Forecast System (GFS) 200 and 850 hPa horizontal wind analyses, the CIMSS approach utilizes a local three-dimensional analysis of high-density, satellite-derived atmospheric motion vectors (AMVs) to calculate horizontal wind analyses at mandatory levels with much less dependence on the 6-h GFS forecast as a background than does the SHIPS technique. Then the VWS is the vector difference between the pressure-weighted mean wind fields in the 150–300-hPa and the 700–950-hPa layers. Both approaches use a vortex-filtering methodology in the final VWS estimate.

Some limitations of only having these VWS products at 6-h intervals will be described in section 2. A special VWS dataset prepared by CIMSS based on AMVs at 15-min intervals (Velden and Sears 2014) will then be examined. Some unique observations from the Tropical Cyclone Intensity (TCI-15) field experiment (Doyle et al. 2017) will be utilized in section 3 to infer how internal processes contributed to the maintenance of Hurricane Joaquin following the interruption of its rapid decay. A summary and discussion will be presented in section 4.

2. Contributions of environmental vertical wind shear

The key result from Jorgensen (2017) was that both the 6-h SHIPS and the CIMSS analyses had large magnitudes of VWS at the onset of rapid decay, and then decreased

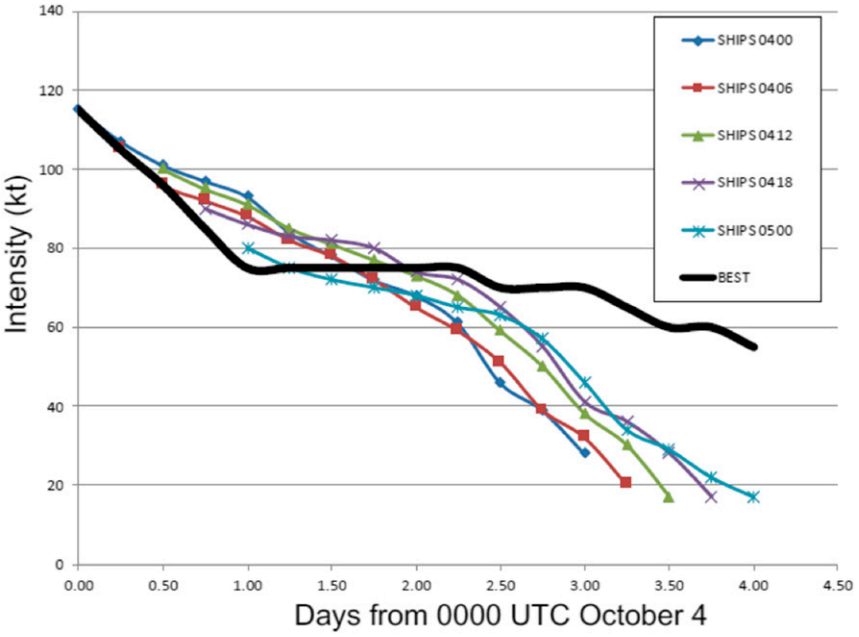

FIG. 1. Real-time SHIPS intensity forecasts (kt) for Hurricane Joaquin each 6 h from 0000 UTC 4 Oct to 0000 UTC 5 Oct (see line color definitions in upper right) vs the National Hurricane Center best-track intensities from Berg (2016) in black.

in magnitude to ''moderate'' [defined as 5–10 m s^{-1} by Corbosiero and Molinari (2002)] VWS during the period of constant intensity (Fig. 2a). Rios-Berrios and Torn (2017) also examined environmental factors that influenced intensity changes under moderate VWS (which they defined as 4.5–11 m s^{-1}), but they only compared intensifying versus steady-state events and not the weakening events such as in Hurricane Joaquin. Note that there are considerable differences in magnitudes and analysis-to-analysis variability in Fig. 2a, especially with the SHIPS technique. Although the SHIPS intensities in Fig. 1 start at the warning intensities, the anomalously small SHIPS VWSs at 0000 and 1800 UTC 4 October in Fig. 2a may have contributed to the SHIPS underforecast of the rapid weakening of Joaquin following those times (Fig. 1). By contrast, the CIMSS technique has a larger peak magnitude and has a much smoother time evolution from 1800 UTC 3 October to 0600 UTC 5 October.

Since the remainder of the environmental variables examined by Jorgensen (2017) did not provide a definite contribution to the interruption of the rapid decay of Joaquin, only a brief summary will be provided here. Because the real-time SHIPS SSTs steadily decreased from 29.8°C at the time of maximum intensity to 26.7°C at 1200 UTC 5 October (Jorgensen 2017, Fig. 16), this environmental factor cannot be connected to the sudden interruption of the rapid decay around 0000 UTC 5 October. Various authors (e.g., Bosart et al. 2000; Rappin et al. 2011) in addition to Hendricks et al. (2010) have related intensity increases to the local upper-tropospheric divergence. In the case of Hurricane Joaquin, Jorgensen (2017, Fig. 17) documented a continued steady decrease in the 200-mb (1 mb = 1 hPa) divergence from a peak

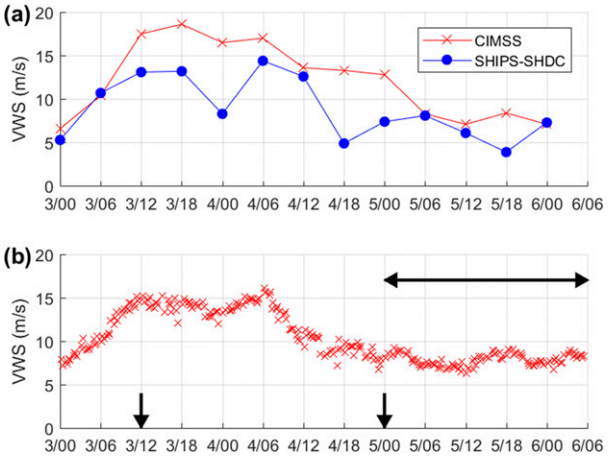

FIG. 2. (a) Time series of the 6-hourly SHIPS (SHDC; deep-layer shear with vortex removed) and CIMSS deep-layer VWS magnitudes (m s^{-1}) from 0000 UTC 3 Oct (3/00) to 0600 UTC 6 Oct (6/06). (b) As (a), but for time series of CIMSS VWS magnitudes (m s^{-1}) based on the special set of 15-min interval AMVs. The vertical arrow on the left indicates the time of maximum intensity of Joaquin, and on the right indicates the time of interrupted rapid decay which is followed by a 30-h period of constant intensity (horizontal arrow).

value at the time of maximum intensity (1200 UTC 3 October) through the period of constant intensity until 0000 UTC 6 October. Hendricks et al. (2010) found decreases in the midlevel (700–500 mb) relative humidity in the tropical cyclone (TC) environment were correlated with weakening. However, Jorgensen (2017, Fig. 18) documented that the midlevel relative humidity around Hurricane Joaquin was a maximum during the rapid decay and was decreasing rapidly during the subsequent period of constant intensity. Although Jorgensen (2017, Fig. 18) did find a temporary increase in environmental relative vorticity at the time of the interrupted rapid decay (0000 UTC 5 October), a rapid decrease in relative vorticity was analyzed during the subsequent period of constant intensity.

Some reasons are suggested for the large 6-h SHIPS VWS variability in Fig. 2a from 1800 UTC 3 October to 0000 UTC 4 October to 0600 UTC 4 October and again from 1200 UTC 4 October to 1800 UTC 4 October to 0000 UTC 5 October in comparison to the relatively small 6-h variability of the CIMSS VWSs. During 2015, the SHIPS VWS was being calculated based on background 6-h GFS forecasts and included hourly AMVs (thus utilizing ±30-min images), but only at the 6-h synoptic times, which may explain the 6-h variability. Furthermore, the AMVs incorporated in the data assimilation for the GFS had been thinned to be appropriate for the effective GFS horizontal grid resolution. Finally, the quality control criteria between the AMV magnitudes and directions were being applied relative to the wind fields in a model-predicted TC vortex that had been relocated from the 6-h GFS forecast position to the observed position. If those AMVs indeed reflect the real Joaquin vortex structure and outflow, the AMVs may easily have been rejected in the quality control step because of their significant deviations from the GFS vortex structure and outflow.

By contrast, the 6-h CIMSS VWSs in the region of Joaquin primarily depend on carefully quality controlled AMVs (Velden and Sears 2014) and were less influenced in the region of Joaquin by background model-predicted GFS wind fields. It was these more smoothly varying 6-h CIMSS VWSs that motivated the reprocessing of the AMVs at 15-min intervals to create a higher temporal resolution VWS dataset. Note that in this reprocessing the GFS background tolerance was relaxed to allow more vectors not in agreement with the smoother GFS background flow.

The description of this VWS dataset based on AMVs at 15-min intervals will focus on the period of interrupted rapid decay and the subsequent period of constant intensity of Hurricane Joaquin (Fig. 2b). In these VWS calculations, the TC vortex has been removed to a radius of 600 km in the 150–300-mb layer and to 800 km in the 700–950-mb layer wind analyses. Note that between 0000 and 1200 UTC 3 October as Joaquin was intensifying to its maximum intensity of 135 kt, the VWS magnitude was consistently increasing from a moderate value of 7 to 15 m s^{-1}. From 1200 UTC 3 October to 0600 UTC 4 October, the VWS remained at very large magnitudes of 14–15 m s^{-1}, and the intensity of Joaquin deceased 30 kt in that 18-h period (Table 1).

The key improvement in these 15-min VWSs relative to the 6-h CIMSS VWSs in Fig. 2a is in the timing of the decrease from these very large VWS magnitudes at 0600 UTC 4 October to a moderate value of 8 m s^{-1} by 1500 UTC 4 October. At this critical time leading up to the interrupted rapid decay at 0000 UTC 5 October, the 6-h CIMSS VWS values at 1800 UTC 4 October and 0000 UTC 5 October are 12–13 m s^{-1}, which at least at 1200 UTC 4 October may be related to the use of the GFS fields as the background at this synoptic time as the SHIPS VWS was also 13 m s^{-1}. Whereas the 15-min VWSs were in the moderate range of 7–9 m s^{-1} from 1500 UTC 4 October and throughout the subsequent period of constant intensity, the 6-h CIMSS VWSs were not in the moderate range until 0600 UTC 5 October. In conclusion, these high temporal resolution CIMSS VWSs at 15-min intervals demonstrate the environmental VWS may vary on the same time scales as occurred during the interrupted rapid decay of Joaquin, and yet then have consistent, nearly constant, moderate VWS during the subsequent period of constant intensity.

These 15-min CIMSS VWSs can also be plotted in the horizontal to examine the relationships between the VWS distribution and the intensity changes (Fig. 3). At 1815 UTC 2 October (Fig. 3a), Joaquin had begun to move away from the Bahama Islands at a translation speed of 3.45 m s^{-1} toward 26° from north (Table 2), which is based on the Creasey and Elsberry (2017) Zero Wind Center (ZWC) technique that utilizes High Definition Sounding System (HDSS; Black et al. 2017) dropwindsondes. That is, an accurate determination of the ZWCs at two successive center overpasses during a NASA WB-57 mission provides a highly accurate translation speed and direction during the period between the two center overpasses. The CIMSS VWS averaged over 500 km at 1815 UTC 2 October was 6 m s^{-1} from the northwest (315°; Table 2). While the center of Joaquin (red dot in Fig. 3a) was just to the east of an extended south-to-north region of 2–3 m s^{-1} VWS, farther to the east was a region of northwesterly VWS exceeding 20 m s^{-1} that was also contributing to the area-averaged VWS. Thus, the dominant synoptic feature contributing to the VWS over Joaquin appears to be an upper-tropospheric trough to the east.

At 1815 UTC 3 October (Fig. 3b), Joaquin was rapidly translating at 8.75 m s^{-1} toward 57° from north, and the

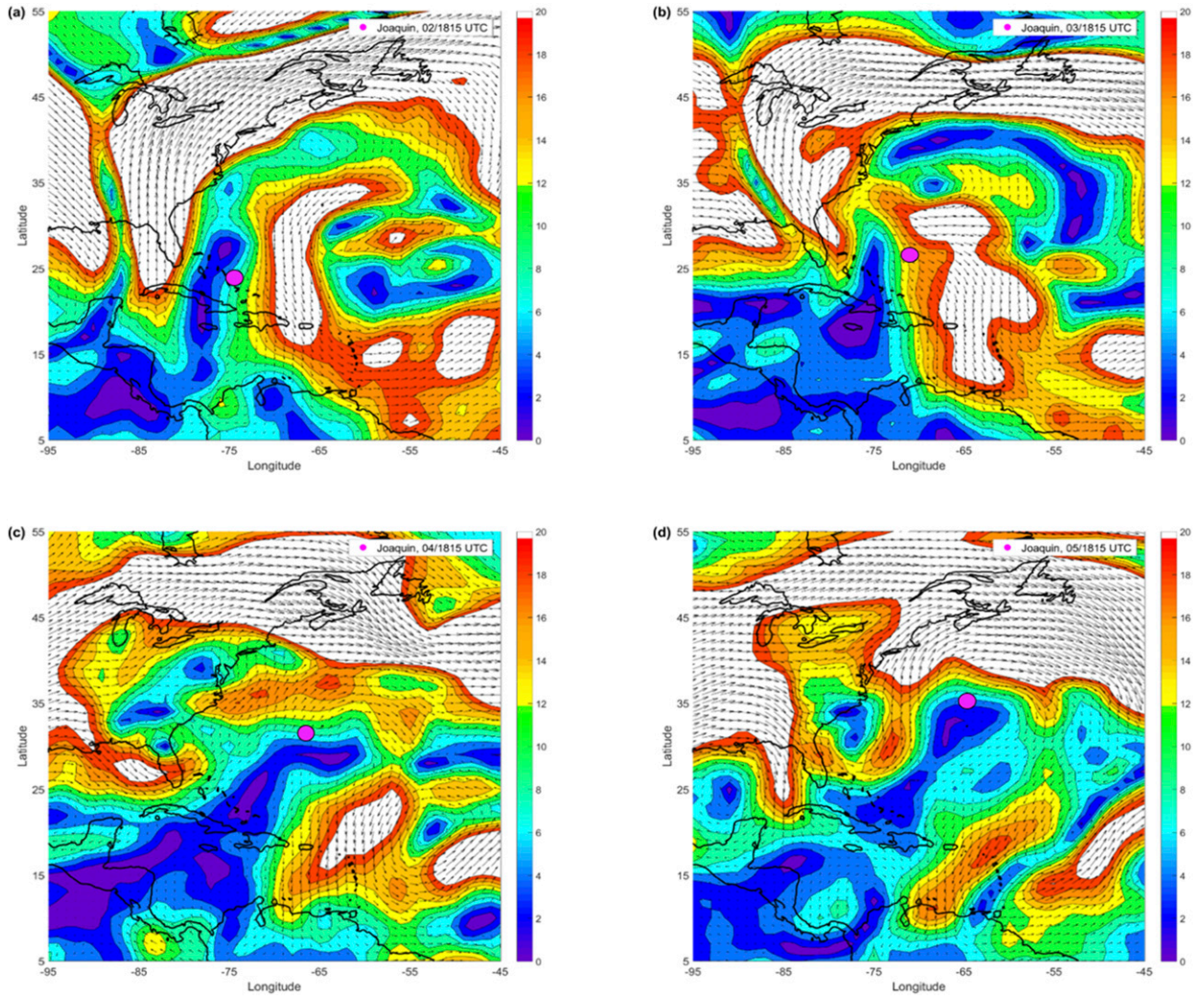

FIG. 3. Positions (red dots) of Hurricane Joaquin depicted in the CIMSS VWS vector analyses ($m\,s^{-1}$; color contour scale on right with values larger than $20\,m\,s^{-1}$ in white) at (a) 1815 UTC 2 Oct when Joaquin was at 110 kt, (b) 1815 UTC 3 Oct when Joaquin was starting to rapidly decay, (c) 1815 UTC 4 Oct just prior to the interrupted rapid decay, and (d) 1815 UTC 5 Oct during the period of constant intensity.

CIMSS VWS was very large at $15\,m\,s^{-1}$ from the west-northwest (305°; Table 2). It is clear from Fig. 3b that this large VWS was primarily associated with the north-to-south band of large ($>20\,m\,s^{-1}$) VWS just to the east of Joaquin. Thus, at 1815 UTC 3 October Joaquin was rapidly moving to the northeast while still at 130 kt intensity even though it was being affected by large VWS. However, this large VWS that was associated with an upper-tropospheric trough may be considered to be a "good trough interaction" in that the Joaquin outflow to the northeast and east could be accelerated toward the lower pressures in that trough.

The rapidly changing environmental conditions affecting Joaquin continued at 1815 UTC 4 October as the translation speed decreased to $4.6\,m\,s^{-1}$ and turned toward 23° from north, and the CIMSS VWS had decreased to $9\,m\,s^{-1}$, but now was from the west-southwest (245°; Table 2). Note in Fig. 3c that Joaquin was within a gradient region between very large VWS on the northern side and near-zero VWS on the southern side. As Berg (2016) indicated, Joaquin was also being influenced during the rapid decay by the VWS associated with an upper-tropospheric trough to the west over northern Florida (Fig. 3c), and these environmental influences are reflected in the CIMSS VWS analyses. However, this VWS is clearly not uniform across the width of the Joaquin circulation, as is often assumed in idealized numerical simulations (e.g., Finocchio et al. 2016). Rather, it is highly asymmetric relative to the Joaquin center (Fig. 3c), as in the case studies in Elsberry and Jeffries (1996) and Park et al. (2012). Although Joaquin at 1815 UTC 4 October was in an environment with a moderate area-averaged

TABLE 2. Hurricane Joaquin storm course and speed, vortex tilt magnitude, and azimuthal direction (degrees relative to north) over lower and upper layers of the troposphere from the Creasey and Elsberry (2017) ZWC technique at the times of four WB-57 overpasses of the center, and corresponding CIMSS 15-min VWS magnitudes and directions. Note that the vortex center could not be tracked above 11.5 km on 2 Oct and 10.5 km on 4 Oct.

	Storm course (°)	Storm speed ($m\,s^{-1}$)	Vertical tilt (km)	Azimuth direction (°)	CIMSS VWS magnitude ($m\,s^{-1}$)	Direction (°)
1800 UTC 2 Oct	26	3.45			6	315
1500–11 500 m			12	335		
1800 UTC 3 Oct	57	8.75			15	305
1500–14 500 m			13	199		
1800 UTC 4 Oct	23	4.6			9	245
1500–5500 m			1	00		
5500–10 500 m			32	51		
1800 UTC 5 Oct	64	12.3			8	255
1500–9500 m			5	15		
9500–14 500 m			22	149		

VWS magnitude of $9\,m\,s^{-1}$ (Table 2), much larger environmental VWS just to the north may have contributed to the continued decay to 85-kt intensity at that time (Table 1).

A CIMSS VWS analysis at 1815 UTC 5 October during the subsequent constant intensity of Joaquin around is shown in Fig. 3d. Note that even though Joaquin was translating rapidly ($12.3\,m\,s^{-1}$) to the northeast (Table 2), it continued to be within a gradient region between large environmental VWS to the north and near-zero VWS to the south. Thus, Joaquin had continued to be in a moderate area-average VWS environment of $\sim 8\,m\,s^{-1}$ (Table 2, column 6) that may have allowed it to continue at hurricane intensity (75 kt) even though the underlying SST had decreased to 26.7°C (Jorgensen 2017, Fig. 16).

3. Contributions of internal factors

Internal processes such as vortex tilt in response to these environmental VWS changes and the inner-core temperature anomalies will be illustrated with the unique sets of HDSS dropwindsondes deployed from the NASA WB-57 flying at 60 000 ft (~18 km) over the center of Hurricane Joaquin during the TCI-15 field experiment (Fig. 4). Although the two missions of most interest are the third mission on 4 October (Fig. 4, third mission from bottom) just prior to the time of the interrupted rapid decay, and the fourth mission on 5 October that was during the subsequent period of constant intensity, the missions on 2 and 3 October will also be described to provide a broader view of the Joaquin vortex tilt in response to VWS.

a. Vortex tilts through the tropopause

The Creasey and Elsberry (2017) technique for deriving ZWCs is patterned after the well-established technique of Willoughby and Chelmow (1982) that is used for aircraft horizontal eye penetrations, except this unique vortex tilt dataset is derived from ZWCs from the average wind directions over 1-km layers every 200 m as the HDSS sondes descended from 60 000 ft to the ocean surface. Typically, wind directions from a sequence of three HDSS sondes in (or near) the eye are utilized. The intersections of the normal vectors to these wind directions then define the ZWCs at 200-m spacing in the vertical (Fig. 5, small circles). These ZWCs provide the Joaquin vortex tilts from 1.5 km (technique only applies above the boundary layer wind turning) to as high in the troposphere as the vortex can be defined (Table 2).

At 1800 UTC 2 October when Joaquin had an intensity of 110 kt (Table 1), the vortex tilts are based on a combination of the ZWCs from three HDSS soundings deployed between 1742:00 and 1743:58 UTC along the inbound flight track and three soundings between 1834:20 and 1835:39 UTC during the second eye-crossing (Fig. 5a). These two sets of ZWCs are internally consistent with a near-vertical inner core of the Joaquin vortex between 1.5 and 11.5 km. Above this level, the three ZWCs from the first eye-crossing become so diverse that it is difficult to detect a vortex center. The three pairs of HDSS soundings during the second eye-crossing also have diverse ZWCs that originate at higher and higher elevations, tilt toward the west, but then also become too diverse to confidently detect a vortex center. If these diverse ZWCs may be interpreted as swirls associated with mesoscale vortices on the inner side of a vertically expanding eye, then an essentially vertical vortex may only exist between 1.5 and 11.5 km at 1800 UTC 2 October (Table 2).

At 1800 UTC 3 October Joaquin's intensity had decreased to 130 kt just 6 h after the peak intensity of 135 kt (Table 1). The ZWCs indicate the vortex was vertical between 1.5 and 11.5 km and then had a tilt of 11 km to the south between 11.5 and 14.5 km (Fig. 5b). Although there

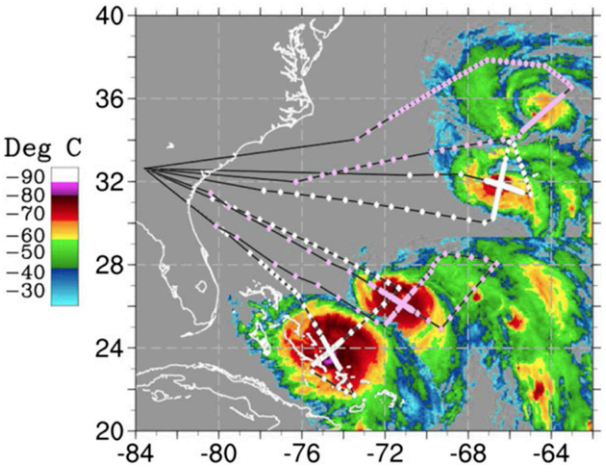

FIG. 4. NASA WB-57 flight tracks (solid lines) and dropwindsonde deployment locations (diamonds) for the four TCI-15 missions in Hurricane Joaquin at approximately 1800 UTC 2–5 Oct from bottom to top, overlaid on color-enhanced GOES infrared satellite imagery, with each image centered on the time the aircraft was over the storm (Doyle et al. 2017). The third mission on 4 Oct, when Joaquin was near 32°N, was just prior to the time of the interrupted rapid decay, and the fourth mission on 5 Oct was during the period of constant intensity.

are also some small oscillations about the vertical inferred from the ZWCs in the middle troposphere, the Joaquin vortex at 1800 UTC 3 October will be considered to be near-vertical between 1.5 and 14.5 km (Table 2).

By 1800 UTC 4 October, Joaquin had rapidly decayed to 85 kt in response to large VWS (Fig. 2). A markedly different vortex structure (Fig. 5c) was diagnosed by Creasey and Elsberry (2017) based on the HDSS soundings. The Joaquin vortex was vertical to within 1 km between 1.5 and 5.5 km but was tilted 32 km between 5.5 and 10.5 km (Table 2). Above 10.5 km, the few ZWCs became so scattered that it was not possible to detect an inner-core vortex. Since three pairs of HDSS soundings had been examined to detect the vortex, and the vortex tilt was so extreme (32 km in just 5 km), it is highly likely that the upper-tropospheric portion of the vortex above 10.5 km had been removed.

At 1800 UTC 5 October, Joaquin was in the period of constant intensity of 75 kt following the interruption of the rapid decay. Although there was only one center overpass along a south-to-north flight leg (Fig. 4, top mission), the ZWCs define an essentially vertical (5-km tilt) vortex from 1.5 to 9.5 km (Fig. 5d). However, the vortex tilt from 9.5 to 14.5 km is 22 km toward the southeast (149° from north; Table 2). Thus, on 5 October the depth of the vertically oriented vortex is considerably greater than on 4 October, and the overall depth of the vortex is larger—albeit with a strongly tilted vortex above 9.5 km.

b. *Inertial stability of the Joaquin vortex*

The inertial stability of the vortex is a factor in the resilience of the vortex against the effect of the VWSs in Fig. 3. Assuming a Rankine vortex, inertial stability I^2 may be expressed as $I^2 = (f + 2v/r)^2$, where f is the Coriolis parameter and v is the tangential velocity at radius r. Normally, the I^2 is applied to an axisymmetric vortex, which will be more applicable for the vertically oriented segments of Joaquin in Figs. 5a–d and Table 2. Although not tested here, the inertial stability might be calculated just on the upshear side of the vortex in the tilted vortex region. As described in section 2, the large VWSs in the horizontal analyses (Fig. 3) are associated with an upper-tropospheric low to the east of Joaquin on 2 October and then the upper-tropospheric trough to the west and northwest on 3–5 October, and thus these VWSs are concentrated in the upper troposphere.

The premise is that the VWS associated with these synoptic circulations that extend over Joaquin in the upper troposphere must be resisted by the inertial stability if the Joaquin vortex is to remain vertical. Where the vortex inertial stability is not sufficient to resist the strong penetrating upper-tropospheric flow associated with the large VWS, the top of the vortex (and thus the warm core aloft) will be dispersed downstream. Below this level at which the vortex flow is dispersed, the vortex will be tilted down-shear to a depth in the middle troposphere at which the larger inertial stability of the vortex in the lower troposphere is sufficient to resist the smaller VWS in the lower troposphere. Below that level, the TC vortex should be vertical.

It is very difficult to establish whether a series of HDSS dropwindsondes along a WB-57 flight path over the Joaquin center has detected the maximum wind speed $V_{\max,}$ and with only two center overpasses it is difficult to calculate the azimuthal-mean $V_{\max.}$ To estimate the inertial stability, first the total storm-relative horizontal velocity vector was decomposed into radial and tangential components about the ZWC. Then for all HDSS dropwindsondes between 40 km $< r <$ 100 km, the I^2 values were averaged at each vertical level to obtain an approximation of the I^2 vertical profile for each of the four Joaquin missions (Fig. 6). Note that for the missions on 2 and 3 October, the larger values of inertial stability continued higher in the troposphere than for the 4 and 5 October missions. The significant reduction in inertial stability aloft between 10 and 15 km on 4 October is considered to have been a persisting effect of the strong vertical wind shear that had impacted Joaquin during the rapid decay period (Fig. 2). At 1800 UTC 5 October during an extended period of moderate vertical wind shear, the Joaquin vortex was

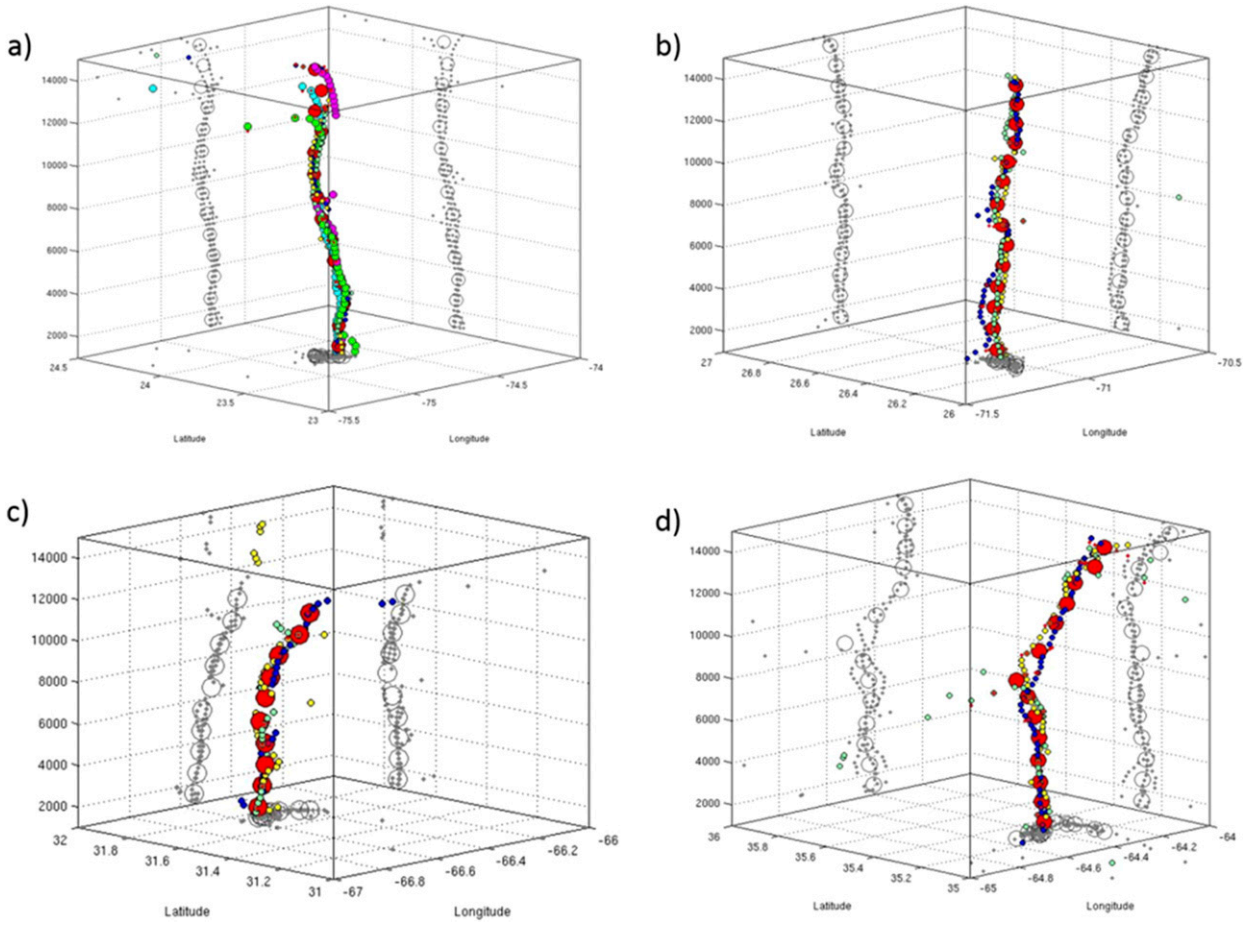

FIG. 5. Hurricane Joaquin vortex tilt between 1.5 and 14.5 km in storm-relative coordinates derived from the changes in the HDSS sonde average wind directions over 1-km layers (large red circles) and at intermediate 200-m elevations (small circles, with yellow, green, and blue circles indicating the three HDSS sondes utilized) during NASA WB-57 overpasses at (a) 1800 UTC 2 Oct, (b) 1800 UTC 3 Oct, and (c) 1800 UTC 4 Oct from Creasey and Elsberry (2017), and at (d) 1800 UTC 5 Oct. The gray circles are the projections of the colored circles onto two-dimensional planes of latitude and longitude vs height.

nearly vertical to 9.5 km (Table 2) but was tilted above that level.

c. *Intensity changes in response to VWS impacts on tilted vortex structure*

A tropical cyclone is a warm-core circulation in which there is an approximate gradient thermal wind balance between the vertical variation of the maximum winds and the virtual temperature gradient across the eyewall at that level. Thus, the vortex structure in the vertical direction should be related to the vertical variation of the temperature anomaly within the eye relative to the environmental temperature. From the hydrostatic equation, the minimum SLP in the eye is related to a downward integration of the pressure-weighted temperature anomaly in the column, where it is assumed the tropopause is horizontal. It is via this thermodynamic and dynamic pathway that the intensity (minimum SLP or maximum surface wind speed) changes may be related to the tilted vortex structure in response to the environmental VWS.

The temperature anomaly within the eye region relative to the near-environment of Joaquin was calculated in each mission by averaging the temperature profiles from the HDSS soundings within 20 km of the center and subtracting the average of the temperature profiles of the HDSS soundings along the inbound and outbound flight legs within 300–400-km radius from the center. Note that the continued presence of a cold upper-tropospheric trough to the west during each mission may contribute to the warm anomalies aloft being larger than if the Dunion (2011) standard atmosphere had been utilized. The raw HDSS temperatures were interpolated to a uniform grid in the vertical direction with a spacing of 500 m. Because no vertical averaging of the temperature profiles was applied before interpolation, the temperature anomaly profiles are slightly noisy (Fig. 7).

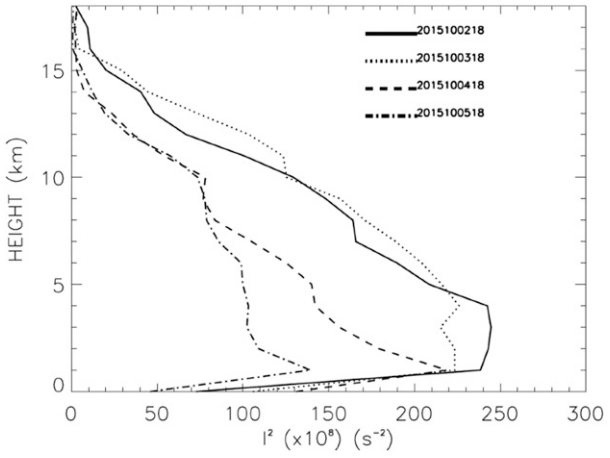

FIG. 6. Inertial stability of the Joaquin vortex as a function of height at 1800 UTC 2 Oct, 1800 UTC 3 Oct, 1800 UTC 4 Oct, and 1800 UTC 5 Oct (see legend for line definitions).

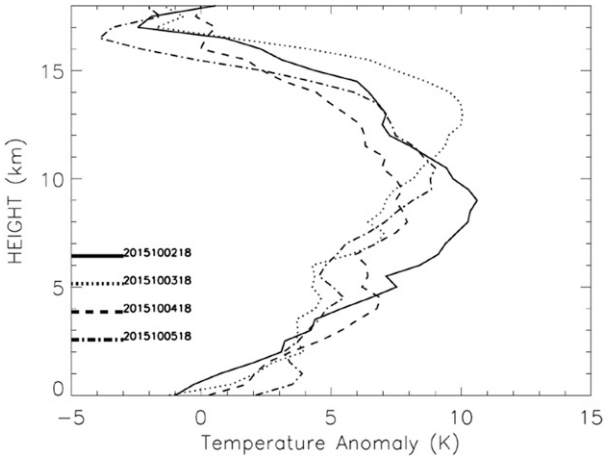

FIG. 7. As in Fig. 6, but for inner-core temperature (°C) anomalies based on HDSS soundings within 20-km radius of the center location and relative to the soundings along the inbound and outbound flight legs within 300–400-km radius from the center.

Even though Joaquin was a 110-kt hurricane at 1800 UTC 2 October (Table 1), the maximum temperature anomaly of 10.5°C was between 7.6 and 10 km rather than in the upper troposphere (Fig. 7, solid black line). From the thermal wind balance equation, below the maximum in this warm core the cyclone tangential winds are rapidly increasing toward the surface. Above the maximum in this warm core, the tangential winds are becoming less cyclonic with increasing height. A decreasing cyclonic flow up to and beyond 11.5 km would be consistent with the difficulty of detecting a ZWC from HDSS soundings above 11.5 km (Fig. 5a, Table 2). Even though the ZWCs indicated a vertical column only up to 11.5 km (Fig. 5a, Table 2), the large magnitude warm core between 7 and 10 km was evidently capable of sustaining a 110-kt hurricane.

At 1800 UTC 3 October when Joaquin had an intensity of 130 kt (Table 1), the temperature anomaly profile represents a deep and thick warm core between approximately 8 and 15 km (Fig. 7, dotted black line). Even though the cyclonic winds are decreasing with increasing height, the ZWCs were well defined to 14.5 km. Because these ZWCs indicated this deep and thick warm core was essentially vertical, this warm column appears to be consistent with the 130-kt intensity.

The positive temperature anomaly at 1800 UTC 4 October (Fig. 7, dashed black line) rapidly increased from near the surface to around 4 km, but then decreased before again increasing more slowly up to 8 km. This less deep and weaker warm core is from the thermal wind equation consistent with a weaker cyclonic vortex at the surface, and Joaquin was near the end of the rapid decay period with an intensity of 85 kt (Table 1). The contribution of a separate warm layer between 9 and 13 km is uncertain, because the radial temperature gradient in this layer does not appear to be concentrated in the eyewall region. That is, no turning of the wind directions in the three HDSS soundings, which would indicate a cyclonic center within the 9–13 km layer, was detected (Fig. 5c). Indeed, the ZWCs indicate a vertical inner-core region from 1.5 to 5.5 km, and then a strongly tilted vortex from 5.5 to 10.5 km (Table 2). A possible association of this vortex tilt structure with the temperature anomalies in Fig. 7 is that the rapidly increasing temperature anomalies up to 5.5 km are within the vertical column, but the slower increasing temperature anomalies up to 9 km are within the tilted vortex tube. The decreasing temperature anomalies above 8.5 km would be consistent with reaching the top of the tilted vortex tube at approximately 10.5 km, and this is also the top level at which the HDSS soundings allowed detection of a ZWC (Fig. 5c, Table 2).

Except for a layer between 4.5 and 6 km, the temperature anomalies at 1800 UTC 5 October were steadily increasing with height to near 9°C at 10.8 km (Fig. 7, dash–dotted line). The warm layer may have extended upward to about 12 km before the temperature anomalies rapidly decreased with increasing heights, which is indicative of a rapidly decreasing cyclonic circulation above that level. Thus, it is reasonable that the ZWCs were still able to detect a cyclonic center up to at least 14.5 km on 5 October. Based on the ZWC analysis, that column of warm air was vertical to 9.5 km and then had a 22-km tilt to 14.5 km (Table 2). With the maximum temperature anomaly at 10.8 km relative to an environment that is progressively cooler compared to this poleward moving storm, it is consistent that

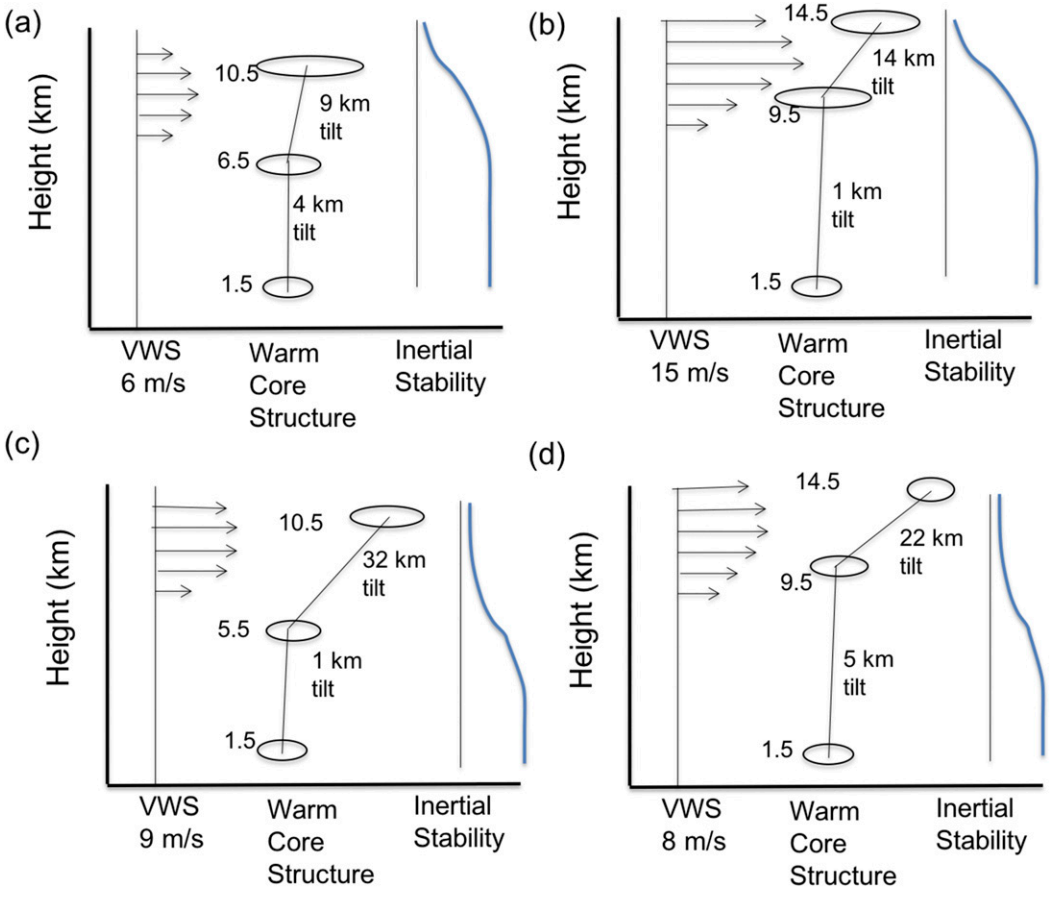

FIG. 8. Summaries of the VWSs that are associated with a typical tropical upper-tropospheric wind profile (schematic on left side) interacting with the TC vortex inertial stability profiles (Fig. 5; schematics on the right) leading to the vortex and warm core tilts from Table 2 (center schematics) for the four WB-57 missions during TCI-15 on (a) 2 Oct, (b) 3 Oct, (c) 4 Oct, and (d) 5 Oct as illustrated in Fig. 3. The ellipses are schematic representations of eye sizes increasing with elevation, except the upper ellipsis in (d) is highly uncertain as Joaquin is becoming extratropical while still maintaining 75-kt intensity.

Hurricane Joaquin could be maintaining an intensity of 75 kt at 1800 UTC 5 October (Table 1) even though the SST was only 26.7°C (Jorgensen 2017, Fig. 16).

d. *Summaries of the VWS impacts on Joaquin vortex structure and intensity*

While other environmental factors may also be affecting the intensity, summaries of the relationships of these vortex tilts to the environmental VWS and the associated impact on the intensity [V_{max} and/or minimum sea level pressure (MSLP)] via the vertical extent and magnitude of the warm core are schematically illustrated in Fig. 8 for the four WB-57 missions. At 1800 UTC 2 October during the first WB-57 mission (Fig. 4, bottom) when Joaquin was at 110 kt (Table 1) and moving at 3.45 m s^{-1} toward 26° (Table 2, columns 2 and 3), a schematic of a typical tropical upper-tropospheric wind profile is shown on the left in Fig. 8a that would be consistent with a moderate VWS magnitude of 6 m s^{-1} at that time (Table 2). A schematic of the inertial stability at that time from Fig. 6 is illustrated on the right in Fig. 8a. Recall that the maximum Joaquin warm core was at least 9°C between 7 and 10.5 km (Fig. 7), and the upper-most level at which the vortex tilt could be calculated was 11.5 km (center schematic in Fig. 8a). Without the benefit of HDSS soundings from an earlier NASA WB-57 mission on 1 October when Joaquin was more intense, it is difficult to explain why the Joaquin V_{max} had decreased 10 kt in the last 18 h (Table 1). As the V_{max} decreased, the inertial stability in the Joaquin vortex presumably also decreased, and thus the resistance to the VWS would also have decreased.

In the premise for this study (section 3b), the depth over which the upper vortex is tilted will increase until a balance is achieved between the VWS magnitude and the inertial stability. The hypothesis is that an equilibrium level exists at which the environmental VWS impact is

completely resisted by the inertial stability of the Joaquin vortex. Above this layer the vortex will have some down-shear tilt of the warm core, but below this equilibrium layer the Joaquin vortex will be vertically oriented, and the depth and magnitude of the warm core below the equilibrium level will determine the MSLP and the V_{max}, which are 942 mb and 110 kt at 1800 UTC 2 October (Table 1).

During the next 24 h until the second WB-57 mission, Joaquin had intensified to 135 kt at 1200 UTC 3 October, but had decreased to 130 kt by 1800 UTC 3 October (Table 1) when Joaquin was moving at 8.75 m s^{-1} into an extreme environmental VWS of 15 m s^{-1} (Table 2). Nevertheless, the vortex tilt from 1.5 to 9.5 km was only 1 km, and it was only between 9.5 and 14.5 km that a tilt of 14 km was diagnosed (Fig. 8b). In terms of the hypothesis, the deep layer from 1.5 to 9.5 km with larger inertial stability in Joaquin at 130 kt was able to resist the large VWS, but at the top of the vortex where the flow changes from cyclonic rotation to radial outflow the inertial stability is zero and the vortex is tilted down-shear. Even though the deep warm core could be considered to be vertically oriented to 14.5 km (Fig. 8b) and thus was able to temporarily sustain the 130-kt intensity, the process of removing the warm core at the top of Joaquin had begun. Since the environmental VWS remained at 15 m s^{-1} at least until 0600 UTC 4 October (Fig. 2b), the cycle of removing the largest magnitude warm core at the top, the MSLP rising, V_{max} decreasing, and inertial stability in the vortex decreasing was in place to rapidly decay Joaquin.

By the time of the third WB-57 mission at 1800 UTC 4 October, Joaquin had moved into a different environment of moderate VWS of 9 m s^{-1} and the translation had slowed to 4.6 m s^{-1} (Table 2). However, the vortex warm core was only vertical from 1.5 to 5.5 km (Fig. 8c) and the extreme 32-km tilt of the warm core between 5.5 and 10.5 km would have contributed little to the MSLP, which had risen to 958 mb. With a corresponding decrease in V_{max} to 85 kt, the inertial stability of the vortex had decreased so that even a moderate VWS would continue the rapid decay (10 kt in 6 h) until it was interrupted at 0000 UTC 5 October (Table 1).

The fourth WB-57 mission was in Joaquin around 1800 UTC 5 October, which was during the period of constant intensity of 75 kt even though Joaquin had recurved to 35.3°N (Table 1). However, Joaquin had continued to be in a moderate VWS environment and the vortex warm core was essentially vertical from 1.5 km up to 9.5 km, and it was only above that level to 14.5 km that the vortex was sharply tilted by 22 km (Table 2, Fig. 8d). Even though that tilt had displaced the warm core from above the surface center, the maximum warm anomaly at 9.5 km was sufficient to sustain a MSLP of 964 mb and a V_{max} = 75 kt (Table 1). With a relatively large vortex inertial stability to 10 km (Fig. 6, and schematic in Fig. 8d) and a continued moderate VWS, a quasi-equilibrium between the VWS and the inertial stability allowed a constant intensity of 75 kt to be sustained.

4. Summary and discussion

The objective of this study has been to utilize two special TCI-15 datasets to document the environmental factors that interrupted the extreme rapid decay of Hurricane Joaquin around 0000 UTC 5 October, and then to understand how Joaquin could maintain an intensity of 75 kt for 30 h despite overall deteriorating environmental conditions. The 15-min CIMSS VWS dataset was particularly valuable in documenting timing of the decrease from large (~15 m s^{-1}) VWS to moderate (~8 m s^{-1}) values prior to the interruption of the rapid decay period. Furthermore, the VWS spatial analyses illustrate well an important asymmetry relative to the Joaquin center. While the VWS over Joaquin's center was in the moderate range during the period of steady-state 75-kt intensity, much larger VWS existed in the northern part of Joaquin's circulation, and near-zero VWS was present over the southern part. Continuous monitoring of the VWS can now be accomplished from *Himawari-8/-9* over the western North Pacific and *GOES-16* over the Atlantic by processing AMVs at 10- and 15-min intervals, respectively.

The HDSS dropwindsondes deployed from the WB-57 flying at 60 000 ft during the interrupted decay period (4 October) and the constant intensity period (5 October) documented the vortex tilt in response to the VWS structure. Deeper lower-tropospheric layers with near-zero vortex tilt were associated with higher intensities. By contrast, upper-tropospheric vortex tilt in response to large VWS magnitudes was associated with weaker intensities during the four TCI-15 missions. Near-continuous monitoring of the ZWCs, vortex tilts, and inner-core vortex structure over periods of up to 24 h would be possible if the HDSS was mounted on a high-altitude Global Hawk pilotless aircraft.

This study has only diagnosed the relationships of the environmental VWS and the vortex tilts to the intensity changes based on analyses of special TCI-15 datasets. Future studies are needed to examine whether the vortex tilt structures (as inferred from the HDSS observations) in response to the environmental VWS can be predicted by regional models. Such studies will achieve the TCI-15 project objectives to not only understand, but also to predict, the impacts of the TC outflow layer on intensity changes.

Acknowledgments. This study is part of the M.S. thesis of Lt. Adam Jorgensen (USN) at the Department of Meteorology, Naval Postgraduate School. Dave Stettner of CIMSS helped with the reprocessed AMV datasets. Eric Hendricks, Mary Jordan, and Bob Creasey are supported by the Office of Naval Research (ONR) Grant N0001417WX01042, Russell Elsberry by ONR Grant N000141712160, and Chris Velden by ONR GRANT N00014-14-1-0116. Penny Jones provided excellent support in the manuscript preparation.

REFERENCES

Berg, R., 2016: Hurricane Joaquin (AL112015). National Hurricane Center Tropical Cyclone Rep., 36 pp., http://www.nhc.noaa.gov/data/tcr/AL112015_Joaquin.pdf.

Black, P., L. Harrison, M. Beaubuen, R. Bluth, R. Woods, A. Penny, R. W. Smith, and J. D. Doyle, 2017: High-Definition Sounding System (HDSS) for atmospheric profiling. *J. Atmos. Oceanic Technol.*, **34**, 777–796, https://doi.org/10.1175/JTECH-D-14-00210.1.

Bosart, L. F., C. S. Velden, W. E. Bracken, J. Molinari, and P. G. Black, 2000: Environmental influences on the rapid intensification of Hurricane Opal (1995) over the Gulf of Mexico. *Mon. Wea. Rev.*, **128**, 322–352, https://doi.org/10.1175/1520-0493(2000)128<0322:EIOTRI>2.0.CO;2.

Corbosiero, K. L., and J. Molinari, 2002: The effects of vertical wind shear on the distribution of convection in tropical cyclones. *Mon. Wea. Rev.*, **130**, 2110–2123, https://doi.org/10.1175/1520-0493(2002)130<2110:TEOVWS>2.0.CO;2.

Creasey, R. L., and R. L. Elsberry, 2017: Tropical cyclone center positions from sequences of HDSS sondes deployed along high-altitude overpasses. *Wea. Forecasting*, **32**, 317–325, https://doi.org/10.1175/WAF-D-16-0096.1.

DeMaria, M., M. Mainelli, L. K. Shay, J. A. Knaff, and J. Kaplan, 2005: Further improvements to the Statistical Hurricane Intensity Prediction Scheme (SHIPS). *Wea. Forecasting*, **20**, 531–543, https://doi.org/10.1175/WAF862.1.

Doyle, J. D., and Coauthors, 2017: A view of tropical cyclones from above: The Tropical Cyclone Intensity (TCI) experiment. *Bull. Amer. Meteor. Soc.*, **98**, 2113–2134, https://doi.org/10.1175/BAMS-D-16-0055.1.

Dunion, J. P., 2011: Rewriting the climatology of the tropical North Atlantic and Caribbean Sea atmosphere. *J. Climate*, **24**, 893–908, https://doi.org/10.1175/2010JCLI3496.1.

Elsberry, R. L., and R. A. Jeffries, 1996: Vertical wind shear influences on tropical cyclone formation and intensification during TCM-92 and TCM-93. *Mon. Wea. Rev.*, **124**, 1374–1387, https://doi.org/10.1175/1520-0493(1996)124<1374:VWSIOT>2.0.CO;2.

Finocchio, P. M., S. J. Majumdar, D. S. Nolan, and M. Iskandarani, 2016: Idealized tropical cyclone responses to the height and depth of environmental vertical wind shear. *Mon. Wea. Rev.*, **144**, 2155–2175, https://doi.org/10.1175/MWR-D-15-0320.1.

Gallina, G. M., and C. Velden, 2002: Environmental vertical wind shear and tropical cyclone intensity change utilizing enhanced satellite derived wind information. *25th Conf. on Hurricanes and Tropical Meteorology*, San Diego, CA, Amer. Meteor. Soc., 3C.5, https://ams.confex.com/ams/25HURR/webprogram/Paper35650.html.

Hendricks, E. A., M. S. Peng, B. Fu, and T. Li, 2010: Quantifying environmental control on tropical cyclone intensity change. *Mon. Wea. Rev.*, **138**, 3243–3271, https://doi.org/10.1175/2010MWR3185.1.

Jorgensen, A. C., 2017: Factors contributing to the interrupted decay of Hurricane Joaquin (2015) in a moderate vertical wind shear environment. M.S. thesis, Dept. of Meteorology, Naval Postgraduate School, 96 pp., https://calhoun.nps.edu/handle/10945/55632.

Park, M. S., R. L. Elsberry, and P. A. Harr, 2012: Vertical wind shear and ocean heat content as environmental modulators of western North Pacific tropical cyclone intensification and decay. *Trop. Cyclone Res. Rev.*, **1**, 448–457, https://doi.org/10.6057/2012TCRR04.03.

Rappin, E. D., M. C. Morgan, and G. J. Tripoli, 2011: The impact of outflow environment on tropical cyclone intensification and structure. *J. Atmos. Sci.*, **68**, 177–194, https://doi.org/10.1175/2009JAS2970.1.

Rios-Berrios, R., and R. D. Torn, 2017: Climatological analysis of tropical cyclone intensity changes under moderate vertical wind shear. *Mon. Wea. Rev.*, **145**, 1717–1738, https://doi.org/10.1175/MWR-D-16-0350.1.

Velden, C. S., and J. Sears, 2014: Computing deep-tropospheric vertical wind shear analyses for tropical cyclone applications: Does the methodology matter? *Wea. Forecasting*, **29**, 1169–1180, https://doi.org/10.1175/WAF-D-13-00147.1.

Willoughby, H. E., and M. B. Chelmow, 1982: Objective determination of hurricane tracks from aircraft observations. *Mon. Wea. Rev.*, **110**, 1298–1305, https://doi.org/10.1175/1520-0493(1982)110<1298:ODOHTF>2.0.CO;2.

Wood, K., and E. A. Ritchie, 2015: A definition for rapid weakening of North Atlantic and eastern North Pacific tropical cyclones. *Geophys. Res. Lett.*, **42**, 10 091–10 097, https://doi.org/10.1002/2015GL066697.